Article

Valorization of Pineapple Leaf Agro-Residues into Bio-Based Ring-Spun Yarns: Microstructural Mapping and Mechanical Behavior of PALF–Cotton Blends

Nattadon Rungruangkitkrai [1], Thanyachol Apipatpapha [2], Nawarat Chartvivatpornchai [1], Jirachaya Boonyarit [2], Warawut Suphamitmongkol [2], Peeraya Ounu [2], Phakkhananan Pakawanit [3], Roengrut Rujanakraikarn [3,4], Rattanaphol Mongkholrattanasit [5], Rungsima Chollakup [2,*]

[1] Department of Textile Science, Faculty of Agro-Industry, Kasetsart University, Bangkok 10900, Thailand; fagitdr@ku.ac.th (NR); nawarat.char@ku.th (NC)

[2] Kasetsart Agricultural and Agro-Industrial Product Improvement Institute (KAPI), Kasetsart University, Bangkok 10900, Thailand; thanyachol.ap@ku.th (TA); aapjab@ku.ac.th (JB); aapwws@ku.ac.th (WS); peerayaounu721@gmail.com (PO)

[3] Synchrotron Light Research Institute (Public Organization), 111 University Ave, Suranaree, Amphur Muang, Nakhon Ratchasima 30000, Thailand; phakkhananan@slri.or.th (PP); roengrut@slri.or.th (RR)

[4] Department of Control Systems and Instrumentation Engineering, Faculty of Engineering, King Mongkut's University of Technology Thonburi, Bangkok 10140, Thailand

[5] Department of Textile Chemistry Technology, Faculty of Industrial Textiles and Fashion Design, Rajamangala University of Technology Phra Nakhon, Bangkok 10300, Thailand; rattanaphol.m@rmutp.ac.th (RM)

* Correspondence: Rungsima Chollakup, Email: aaprmc@ku.ac.th; Tel.: +66-2-9428-600.

ABSTRACT

Pineapple cultivation generates large quantities of non-food leaf agro-residues that are often discarded or burned, despite their significant potential as industrial crop resources. This study valorized pineapple leaf agro-residues, converting them into bio-based ring-spun yarns by blending pineapple leaf fibers (PALF) with cotton, and elucidated how PALF loading affected the microstructural fiber distribution and mechanical behavior. The PALF were mechanically extracted and dyed with cocoa leaves using ferrous sulfate as a mordant prior to blending with cotton at ratios of 0:100, 20:80, 30:70, and 50:50. Bio-based PALF–cotton yarns (5 and 10 Ne) were produced using a laboratory-scale ring-spinning system and characterized in terms of physical, evenness, and tensile properties. Fiber distribution within the yarn cross-section was mapped using optical microscopy, scanning electron microscopy (SEM), and synchrotron radiation X-ray tomographic microscopy (SRXTM), and

Open Access

Received: 24 Dec 2025
Accepted: 15 Apr 2026
Published: 19 May 2026

quantified using the Index of Blend Irregularity (IBI). IBI values below 1 for cotton and above 1 for PALF confirmed a preferential cotton core and PALF-rich periphery, indicating radially non-uniform fiber dispersion. A 30:70 PALF/cotton blend provided the optimal compromise between strength, elongation, and evenness, while mechanical properties remained broadly comparable across 20–50% PALF, except for increased yarn unevenness at higher PALF contents. Our findings demonstrate the technical feasibility of converting pineapple leaf agro-residues into PALF–cotton bio-based ring-spun yarns, and provide practical design guidelines for low-carbon textile products derived from industrial crop residues.

KEYWORDS: pineapple leaf fibers (PALF); agro-residues; bio-based ring-spun yarns; fiber migration; Index of Blend Irregularity (IBI)

ABBREVIATIONS

PALF, pineapple leaf fibers; SEM, scanning electron microscopy; SRXTM, synchrotron radiation X-ray tomographic microscopy; IBI, Index of Blend Irregularity

INTRODUCTION

Pineapple (*Ananas comosus* (L.) Merr.) is a significant agricultural product in Thailand, with 49,846 hectares dedicated to its cultivation in 2024, positioning the country among the leading global exporters of canned pineapple [1]. However, pineapple harvesting generates substantial quantities of non-food biomass in the form of leaves, rhizomes, and stems. Pineapple leaves contribute 37.5 tons of waste per hectare, amounting to an estimated annual generation of 2.7 million tons [2]. These cellulose-rich residues are often underutilized or managed through field burning, thereby contributing to local air pollution and greenhouse gas emissions. Consequently, there is strong motivation to valorize pineapple leaf agro-residues as industrial crop resources for non-food, bio-based products, particularly sustainable textile intermediates. Despite their abundance, pineapple leaf fibers (PALF) remain largely underutilized at the industrial scale due to challenges associated with fiber stiffness, heterogeneity, and limited compatibility with conventional cotton spinning systems. Addressing these processing barriers is critical to transform PALF from an agricultural residue into a value-added industrial raw material suitable for textile applications.

PALF have attracted considerable interest as a natural, biodegradable lignocellulosic material with potential applications across the automotive, construction, biomedical, furniture, textile, and packaging sectors [3]. In the textile field, PALF have been blended with cotton, polyester, wool, jute, and flax to develop yarns with tailored mechanical and aesthetic properties [4–7]. Prior studies on PALF-based blended yarns have primarily focused on bulk physical and tensile properties, spinnability,

and handling. By contrast, relatively limited attention has been paid to the spatial distribution and migration behavior of PALF within the yarn matrix. This knowledge gap is critical because fiber positioning in blended yarns directly influences yarn strength, abrasion resistance, fabric handle, drape, and visual texture [8,9], thereby affecting the performance and acceptance of bio-based textile products.

Fiber migration, defined as the spatial movement of fibers within the yarn cross-section during spinning, is governed by factors such as fiber fineness, blend ratio, spinning techniques, and surface treatments. Fine and flexible fibers concentrate toward the yarn core, thereby enhancing tensile strength and durability. By contrast, coarser and stiffer fibers migrate toward the periphery, affecting surface texture and fabric feel [8]. Pretreatment methods such as alkaline or enzymatic treatments have been used to improve the quality and spinnability of PALF and remove non-cellulosic components (e.g., pectin and waxes), thereby refining the fiber surfaces and improving mechanical performance [10,11]. Chollakup et al. (2004) [12] further highlighted the broader significance of fiber distribution in natural-fiber-based materials, demonstrating that fiber arrangement significantly influenced soft, greasy and granulous and crumple-like characteristics for tactile description of knitted fabrics especially the different blended fiber in fabrics. These findings collectively reinforce the importance of understanding fiber migration in blended yarns for the design of high-performance, sustainable textile applications.

Blending experiments using semi-worsted spinning systems at the South India Textile Research Association (SITRA) and the Central Sheep and Wool Research Institute have explored PALF blended with coarse animal fibers at a 50:50 ratio, producing yarns of 15 Ne, as well as 30:70 PALF/Merino wool blends yielding 10 Ne yarns via the worsted spinning route. These blends exhibited lower strength and elongation than acrylic yarns, but improved spinning consistency was reported, and fiber conditioning prior to spinning was recommended to optimize PALF for textile applications [13]. Other experimental studies varying PALF content (e.g., 30%, 40%, and 50%) showed that a 30% PALF blend yielded a softer hand, whereas 50% PALF produced coarser and thicker yarns. More advanced enzymatic or alkaline pretreatments enabled higher PALF ratios (up to 80%) while reducing fiber coarseness, thereby allowing the production of finer and softer yarns [14]. These studies demonstrated the technical feasibility of incorporating PALF into yarns, but they also highlighted the need for improved control of fiber distribution to achieve consistent yarn properties.

Recent advances in PALF composites [15] have underscored the potential of PALF in polymer-based systems, while also identifying non-uniform fiber dispersion as a limiting factor for achieving optimal mechanical performance. Duangsuwan et al. (2023) [16] showed that well-aligned PALF in poly(butylene succinate) composites significantly enhanced tensile strength (~45% increase) and thermal stability, thereby

emphasizing the importance of controlled fiber distribution. However, comparable microstructural insights have not yet been systematically extended to PALF-containing textile yarns, where fiber arrangements within the yarn cross-section play a critical role in determining yarn performance.

The visualization and analysis of yarn structure are therefore essential to better understand how the fibers are arranged and migrate within blended yarns. Cross-sectional imaging provides quantitative information on fiber distribution and migration patterns [17,18]. Fiber distribution within the yarn cross-section is influenced by fiber fineness and type, the blending method, yarn count, fiber treatment, and the spinning system [19,20]. Recent studies have used cross-sectional analysis to examine the organization of fibers in the core and sheath regions of yarns [21], while other studies have shown that spinning parameters such as twist level can significantly affect the sensory and mechanical properties of fabrics derived from yarns, including tensile strength, shear, bending, compression, air permeability, and wicking behavior [22].

Previous research has demonstrated the feasibility of using conventional ring-spinning technology to produce PALF-based yarns. Studies in Thailand have successfully blended PALF cut to 40 mm with cotton at ratios of 0:100, 25:75, 35:65, and 50:50, yielding yarn counts of 9.3, 14, and 20 Ne [7], while jute–PALF blends have also shown that the position of PALF within the yarn can strongly affect mechanical properties and appearance [4]. However, despite these advances, a knowledge gap remains in quantitatively understanding the distribution of PALF within ring-spun PALF–cotton blended yarns and how this distribution, particularly along the core–periphery direction, influences yarn characteristics, with limited attention given to how radial fiber migration in PALF–cotton blends governs yarn processability, uniformity, and mechanical reliability—parameters that ultimately determine industrial spinning feasibility and material yield.

A comprehensive understanding of fiber migration behavior is required for the large-scale valorization of PALF. Advanced imaging techniques such as SEM and X-ray micro-computed tomography (micro-CT) have been employed to visualize fiber distribution and migration in textile materials [23]. These methods, in combination with quantitative metrics such as the Index of Blend Irregularity (IBI) and the Migration Index (MI), have enabled high-resolution assessments of fiber dispersion within yarn cross-sections [8,9,17,21].

This study valorized pineapple leaf agro-residues into bio-based ring-spun yarns and addressed the knowledge gap related to PALF–cotton blended yarn microstructure. PALF were mechanically extracted from pineapple leaves, blended with cotton at different ratios, and spun into ring-spun yarns. A natural dyeing step using cocoa leaves and a ferrous sulfate mordant was included to demonstrate the feasibility of sustainable coloration of pineapple leaf fiber yarns using agricultural by-products.

Cocoa leaves contain natural polyphenolic compounds such as tannins and flavonoids, which exhibit a strong affinity for lignocellulosic fibers. The use of ferrous sulfate as a mordant enhances dye fixation through coordination interactions with the hydroxyl groups in cellulose, resulting in more stable coloration. This approach aligned with the sustainability objectives of the study by utilizing renewable dye sources and minimizing the reliance on synthetic dyes, while maintaining chemical compatibility with PALF-based yarns. PALF–cotton yarns were produced using laboratory-scale ring-spinning equipment. Fiber arrangement within the yarn cross-section was analyzed using optical microscopy, SEM, and synchrotron radiation X-ray tomographic microscopy (SRXTM), while fiber migration was quantified through IBI analysis to elucidate the relationship between fiber positioning, mechanical properties, and yarn evenness. This study established the microstructure–property relationships for PALF–cotton ring-spun yarns, and provided design guidelines for integrating pineapple leaf agro-residues, as industrial crop resources, into sustainable textile products to support the development of low-carbon, bio-based yarn systems.

MATERIALS AND METHODS

Materials

The PALF from the smooth cayenne variety, representing agro-residues generated after fruit harvest, was sourced from pineapple plantations in Chiang Rai, Rayong, and Ratchaburi Provinces in Thailand. The leaves were processed using a mechanical decorticator to obtain technical PALF bundles. Commercial cotton fiber, used as the blending partner, was supplied by Erawan Textile Co., Ltd. (Samut Prakan, Thailand). Cocoa leaves for natural dyeing were collected from plantations in Chiang Rai and provided by the garment and apparel A&R Community Enterprise in Chiang Khong District, Chiang Rai Province.

Pineapple Leaf Fiber Preparation and Dyeing Process

The PALF were extracted by decortication and washed twice with water to remove surface impurities, yielding untreated PALF (PALF-U). The PALF-U was then soaked in a silicone softener solution (5 g/L) at 50 °C for 30 min to improve flexibility and spinnability; this material was referred to as softener-treated PALF (PALF-S). The PALF bundles were subsequently cut into short staple fibers with a length of 30–40 mm, suitable for cotton-type spinning.

The chemical compositions of PALF fiber (PALF-U and PALF-S) were determined using standard TAPPI methods. Alpha-cellulose content followed TAPPI T 203 cm-22 (2009) [24], holocellulose followed Browning (1967), extractives followed TAPPI T 204 cm-17 (2009), lignin content followed TAPPI T222 om-21 (2009), and ash content followed TAPPI T211 om-22 (2009) [25–27]. PALF fineness was characterized by measuring the

fiber diameter using an optical microscope (Leica, LM750, Wetzlar, Germany) and converting the diameter values to fiber fineness following the standard method of ISO 1973 [25]. Fiber tenacity and elongation at break were measured using a universal testing machine (Autograph, Shimadzu AGS-5kN, Shimadzu, Japan) in accordance with the standard method of ISO 5079 [28]. Fiber morphology was evaluated from cross-sectional images obtained using the same optical microscope. Fourier transform infrared (FTIR) spectroscopy was employed to identify the functional groups and surface chemical changes in the PALF before and after the softening treatment. The FTIR spectra of untreated PALF (PALF-U) and softener-treated PALF (PALF-S) were recorded using an FTIR Spectrometer (Bruker Tensor 27 spectrometer, Billerica, MA, USA) equipped with an attenuated total reflectance (ATR) accessory. Each sample was placed directly onto the ATR crystal, and sufficient pressure was applied to ensure good contact between the fiber surface and the crystal. The spectra were collected over a wavenumber range of 400–4000 cm^{-1} with a spectral resolution of 4 cm^{-1} and averaged over 64 scans to improve the signal-to-noise ratio.

For the cotton fibers, physical properties (length, uniformity, strength, and related parameters) were assessed using a high-volume instrument (HVI 910, Zellweger Uster, Switzerland) and a Shirley fiber-testing system. Before yarn production, the PALF were dyed with a cocoa leaf extract, giving a distinct natural color to identify PALF within PALF/cotton blended yarn cross-sections. The cocoa leaves were cut into small pieces, homogenized using a blender, and utilized as raw material for dye extraction. The extraction procedure involved mixing the cocoa leaves with distilled water in a 1:10 (w/w) ratio and then boiling the mixture for 1 h. The resulting solution was then filtered to remove solid residues. The extraction condition for the cocoa leaf solution followed a previously reported method described by Rungruangkitkrai et al. (2025) [29]. The PALF were dyed at 100 °C for 1 h in an aqueous cocoa leaf dye bath with a liquor ratio of 1:10 (fiber-to-liquor). After dyeing, a post-mordanting treatment was applied by immersing the dyed PALF in a 5 g/L $FeSO_4$ solution at room temperature to enhance dye fixation and color fastness.

Fiber Blending and Spinning

The dyed PALF (dark brown) was physically blended with undyed white cotton fibers at PALF/cotton mass ratios of 0:100, 20:80, 30:70, and 50:50. The blending of dark brown PALF and undyed white cotton fibers provided a stable color contrast that facilitated clear discrimination between PALF and cotton in yarn cross-sections for imaging-based fiber distribution analysis.

The blended fibers were initially carded to open fiber tufts, remove neps and short fibers, and homogenize the blend. Carding was carried out using a laboratory carding machine (Mesdan Lab, Serial No. 199, Puegnago del Garda, Italy) to produce a lap with a surface mass of 25 g/m^2 and the

lap formation step was repeated twice to improve blending uniformity. The carded web (25 ktex) was drafted into slivers using a laboratory drawing and roving system (Mesdan Lab, Type 3371 Serial No. 55, Puegnago del Garda, Italy). In the first passage, the carded lap was passed through four pairs of rollers under pressure to obtain a drawn sliver of 5.62 ktex (draft ratio of 4.45). Three drawn slivers were then doubled and redrafted with the same draft ratio (4.45), resulting in a final sliver of 3.79 ktex. This system also produced roving before the ring-spinning process. Ring-spinning was performed on a laboratory ring frame (Lab Spinning Machine, Mesdan Lab, Serial No. 440-11, Puegnago del Garda, Italy) equipped with two apron-drafting zones, enabling substantial drafting capability. The maximum PALF loading in the blends was limited to 50% because of the relatively coarse and stiff PALF morphological characteristics. Coarser yarn counts of 5 and 10 Ne (corresponding to 118 and 59 tex, respectively) were selected to ensure a robust spinning performance at high PALF contents. The spinning conditions were set to a spindle speed of 9600 rpm, a ring diameter of 21 mm, a twist factor αNm of 110, and a traveler No. 2 (0.076 g). Under these conditions, the roving was spun into PALF–cotton ring-spun yarns for all the blend ratios.

Characterization of PALF–Cotton Blended Yarns

The physical properties of blended yarns were characterized in accordance with relevant ISO standards. Yarn count was determined following ISO 2060 [30], and yarn twist was measured according to ISO 2061 [30] using a Shirley twist tester (Shirley Developments Limited, Manchester, England). Yarn tenacity and elongation at break were evaluated using an Autograph universal testing machine (Shimadzu AGS-5 kN, Kyoto, Japan) in accordance with ISO 5079 [28]. Yarn unevenness was assessed using an in-house image-based method adapted from the seriplane test for silk filament evenness. Yarns were wound around black cardboard panels (21 cm × 8 cm), and images of the wrapped yarns were digitally processed using smoothing, threshold segmentation, and image enhancement procedures. Thick places and neps per kilometer were then detected and quantified using Leica Application Suite software (LAS 14.12.0, Heerbrugg, Switzerland).

Fiber cross-sections of the PALF–cotton blended yarns were evaluated using three complementary techniques. First, optical microscopy was employed to quantify fiber distribution in the yarn cross-section following the approach of Chollakup et al. (2008) [9].

Blended yarns comprising dyed PALF, undyed cotton fibers, and black polyester support filaments were prepared by inserting the yarn through a 1.25 mm hole in a stainless-steel plate and trimming the cross-sections flush with a razor blade. For each sample, at least 30 cross-sections were imaged using a CCD camera mounted on a Leica Microsystems LM750 optical microscope equipped with a 20× objective lens. The images (2592 × 1944 pixels, RGB format) were processed using ImageJ software (National

Institutes of Health, Bethesda, MD, USA). Disjoint regions along the yarn contours were used to create masks for five concentric zones, which were then applied to identify the PALF. To count the PALF in the yarn cross-sections, intersections between the segmented PALF regions and each concentric zone, from the outermost to the innermost, were identified. Thirty cross-sectional images per blend were analyzed to determine the distribution of each fiber type between the yarn core and outer layers (Figure 1). Image clarity was enhanced by cropping and smoothing the borders using Adobe Photoshop prior to segmentation. Each image was divided into five equal-area concentric zones by successively reducing the central area of each zone by 20%. Fiber types were classified and counted within each zone. The PALF were large, elongated, red-colored entities, whereas the cotton fibers were smaller, circular and white. Image analysis in ImageJ software (National Institutes of Health, USA) was used to obtain fiber counts per zone, and these data were subsequently used to calculate the IBI. This procedure provided a quantitative assessment of fiber migration and radial distribution within the blended yarns, thereby characterizing the degree of blend irregularity.

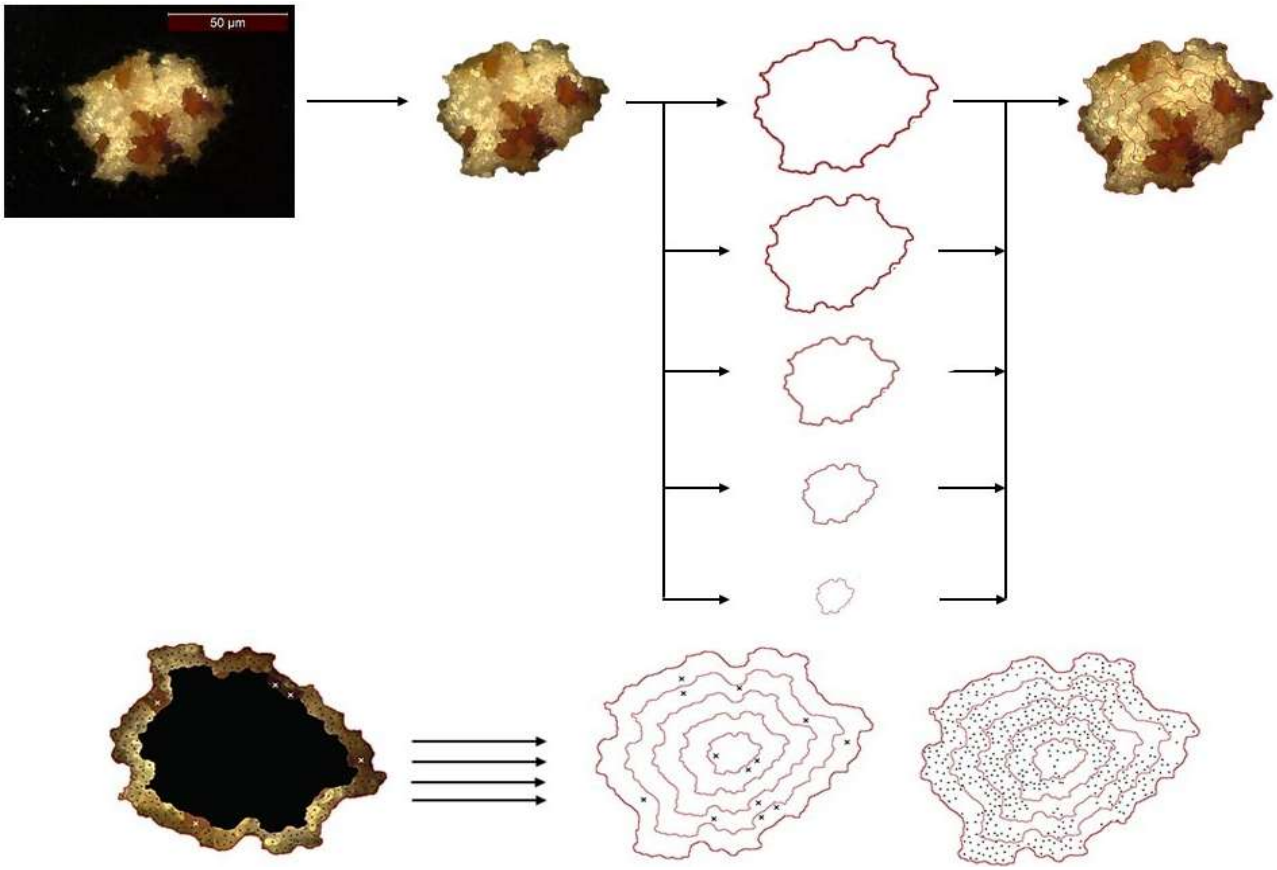

Figure 1. Image processing for counting the number of PALF and cotton fibers for each concentric zone of the optical microscope images.

Second, the yarn cross-sections were examined using SEM. The yarn samples were fractured in liquid nitrogen, sputter-coated with gold, and observed using an SEM instrument (FEI Quanta 450, Hillsboro, OR, USA) operated at an accelerating voltage of 2 kV. The SEM images were processed to divide the yarn cross-sections into five concentric layers, using the same zoning procedure for the optical microscopy images described in Figure 1.

The classification of the PALF and cotton fibers was based on their morphological characteristics. The PALF cross-sections exhibited larger diameters and were more irregular, ribbon-like shapes, whereas the cotton fibers were finer and typically contained a central lumen. Delineating the exact boundaries of each concentric zone in the SEM images was more challenging than in the optical images due to the tendency of the fibers to migrate toward the yarn surface and the complex packing of coarse PALF, but remained feasible for comparative analysis.

Lastly, SRXTM was used to provide three-dimensional information on fiber distribution within the yarn. The SRXTM measurements were performed at beamline 1.2 W using polychromatic X-rays attenuated by a 350 μm aluminum foil. Tomographic projections were recorded using a CMOS detector at a spatial resolution of 0.72 μm. The acquired data were reconstructed using Octopus software, visualized in Drishti, and analyzed for fiber distribution using Python (OpenCV). The image-processing workflow for SRXTM, including reconstruction, segmentation, and zone-based analysis of fiber distribution, is illustrated in Figure 2.

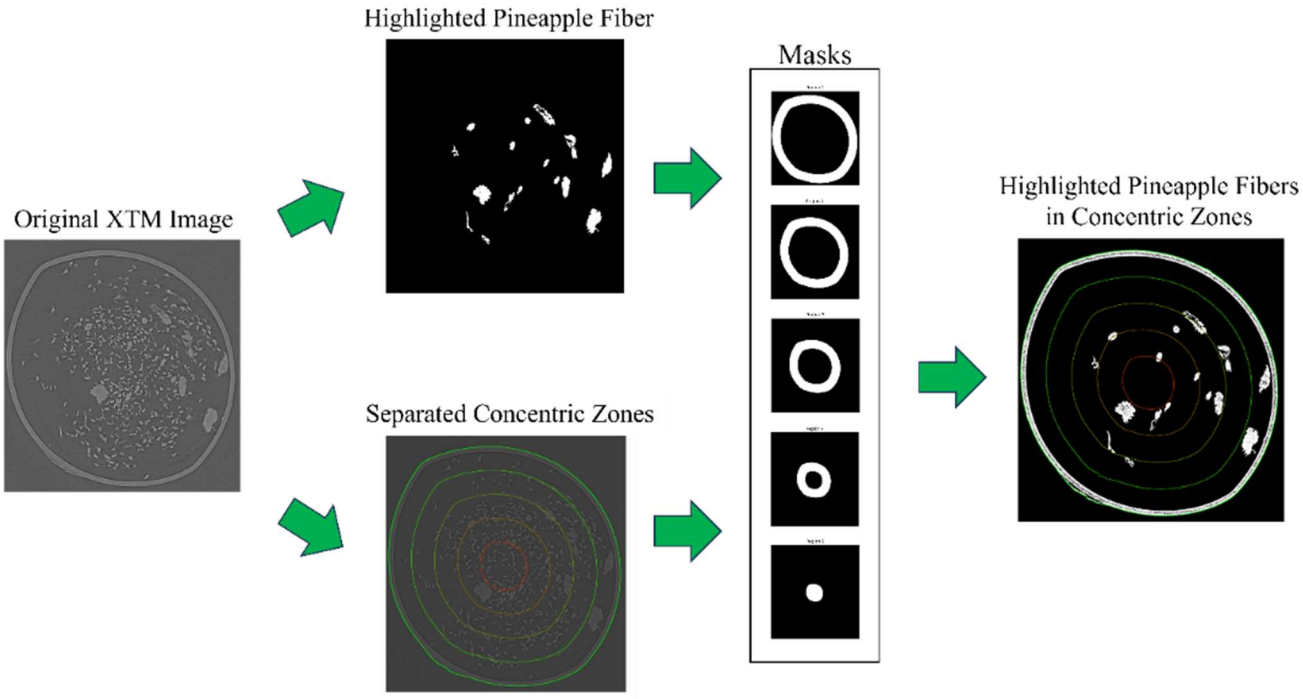

Figure 2. Image processing workflow of X-ray tomography images.

The quantitative composition of the blends was obtained by counting each fiber type in the cross-sectional images. The IBI was used as a dimensionless parameter to evaluate longitudinal blend homogeneity [31,32]. Values close to zero indicate highly uniform, random blending, whereas larger values indicate non-random inhomogeneity. The IBI for a given component w was calculated using Equation (1) [31,32]:

$$\mathrm{IBI} = \sqrt{\frac{1}{n}\sum \frac{(pT_i - W_i)^2}{T_i pq}} \quad (1)$$

where

T_i is the total number of fibers in a given cross-section *i*,

W_i is the total number of fibers of component w in that particular section *i*,

p is the average fraction of component *w* for all sections,

q equals 1 – p and n is the number of yarn cross sections examined.

RESULTS AND DISCUSSION

PALF were produced through multiple processes, including decortication using a fiber extraction machine to obtain untreated PALF (PALF-U). By contrast, the softener-treated PALF (PALF-S) underwent a softening process to enhance fiber dispersion before dyeing with cocoa leaves. PALF-S exhibited improved dispersion, resulting in finer and less cohesive fibers before dyeing. This observation paralleled similar modifications applied to hemp fibers [33], suggesting that softener treatments facilitate better fiber alignment and blending in natural fiber-based textile processing. The cross-sectional view under an optical microscope (Figure 3) demonstrated that soaking pineapple fibers in a silicone-based softener created visible gaps between the fibers [34,35]. SEM images of longitudinal sections of softener-treated PALF revealed a thin silicone layer or agglomerate on the fiber surface that reduced fiber aggregation, enhanced spinning performance in PALF-based blended yarns, and influenced the color absorption behavior of dyed PALF. The surfaces of the untreated fibers were clean and well-defined, with visible fibrillar structures, typical of natural PALF. Similar morphological features were reported for silicone-treated natural fibers and textile substrates, where softener residues appeared as surface-bound layers or patches [36].

Table 1 presents the chemical compositions of PALF before and after softener treatment. There were no statistically significant differences between the untreated (PALF-U) and softened (PALF-S) fibers in terms of the main structural components, including cellulose, hemicellulose, and lignin, indicating that the softener treatment did not alter the bulk chemical structure of the fibers. Such behavior was expected, as silicone-based softeners primarily act as surface modifiers rather than penetrating or chemically reacting with the lignocellulosic matrix [37].

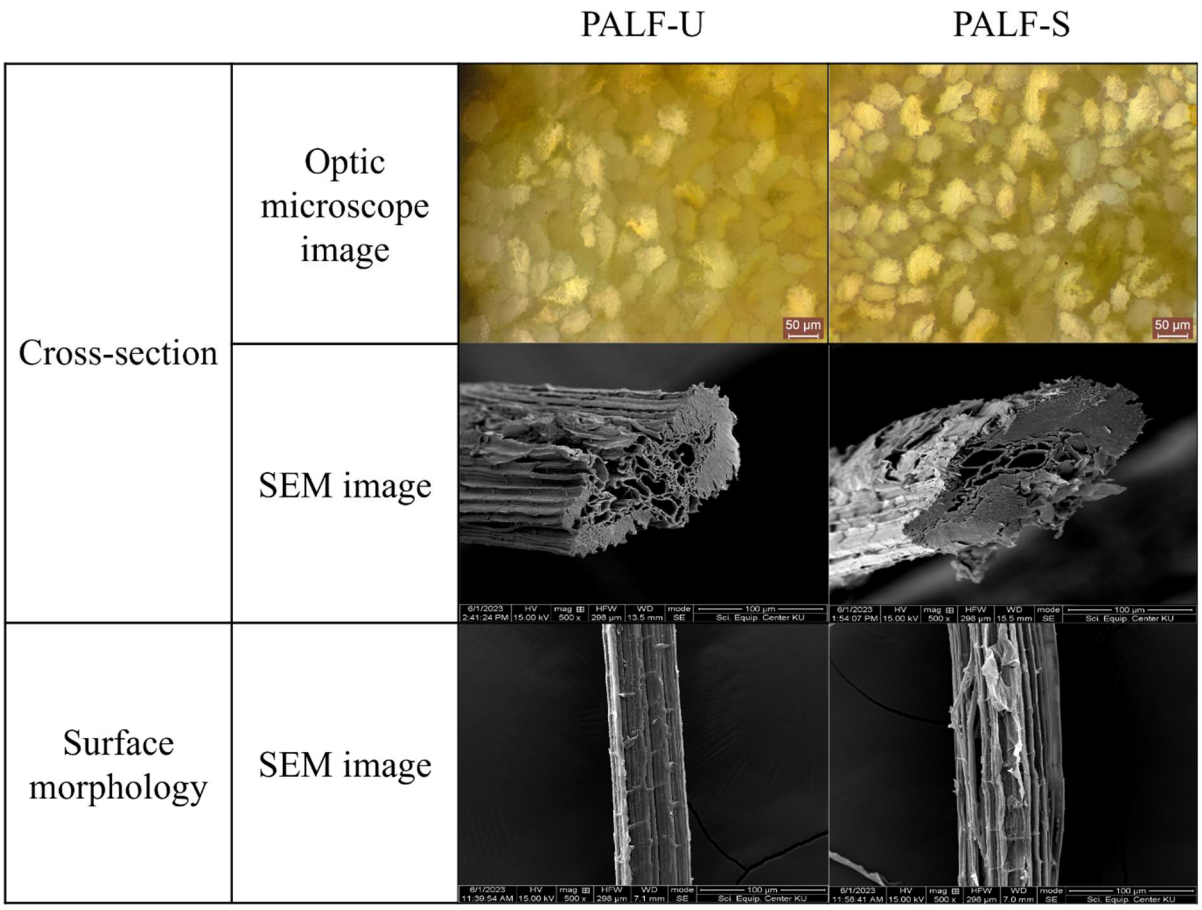

Figure 3. Cross-sectional and surface morphology images of PALF-U and PALF-S observed under an optical microscope at a magnification of 20× and under a scanning electron microscope (SEM) at a magnification of 500×.

A statistically significant increase in the extractives content was observed in softened fibers (PALF-S). These extractives were predominantly soluble in alcohol–benzene mixtures, commonly used to quantify non-polar components such as waxes, oils, lipids, and surface-deposited finishing agents [38]. The elevated extractive contents in PALF-S were attributed to the silicone-based softeners deposited on the fiber surface.

The FTIR spectra of the untreated and softener-treated PALF were analyzed to confirm the presence of surface modification (Figure 4). The FTIR spectrum of untreated PALF (PALF-U) exhibited characteristic absorption bands of lignocellulosic fibers. The broad band centered at 3340 cm^{-1} corresponded to O–H stretching vibrations of the hydroxyl groups in cellulose and absorbed moisture. The band at 2910 cm^{-1} was attributed to C–H stretching vibrations of aliphatic $–CH_2$ groups, while the absorption band at 1732 cm^{-1} was assigned to C=O stretching vibrations of the ester and acetyl groups associated with hemicellulose and residual lignin. Bands from 1000 to 1100 cm^{-1} were assigned to C–O and C–O–C stretching vibrations of polysaccharides, typical of cellulose-based fibers.

By contrast, the softener-treated PALF (PALF-S) exhibited additional spectral features that supported the presence of silicone on the fiber surface. A distinct absorption band at 800 cm^{-1}, observed exclusively in PALF-S and absent in the untreated fibers, was attributed to Si–O–Si symmetric stretching vibrations and/or Si–CH_3 rocking modes, well-established diagnostic peaks of silicone materials, particularly polydimethylsiloxane (PDMS) [37,39]. Lignocellulosic components do not exhibit absorption in this region, and the appearance of the ~800 cm^{-1} band provided strong chemical evidence for the presence of a silicone layer on the PALF surface.

An intense band was also observed at around 1030 cm^{-1}, but this region overlapped with the C–O stretching vibrations of cellulose and, therefore, was not considered conclusive evidence for silicone. Nevertheless, the combined presence of the silicone-specific band at ~800 cm^{-1} and the changes in relative band intensities in the fingerprint region supported the successful deposition of silicone softener on the fiber surface. These FTIR results concurred with previous reports on silicone-coated natural fibers and textile substrates, where Si–O–Si vibrations in the low-wavenumber region were used as reliable indicators of silicone finishes [36].

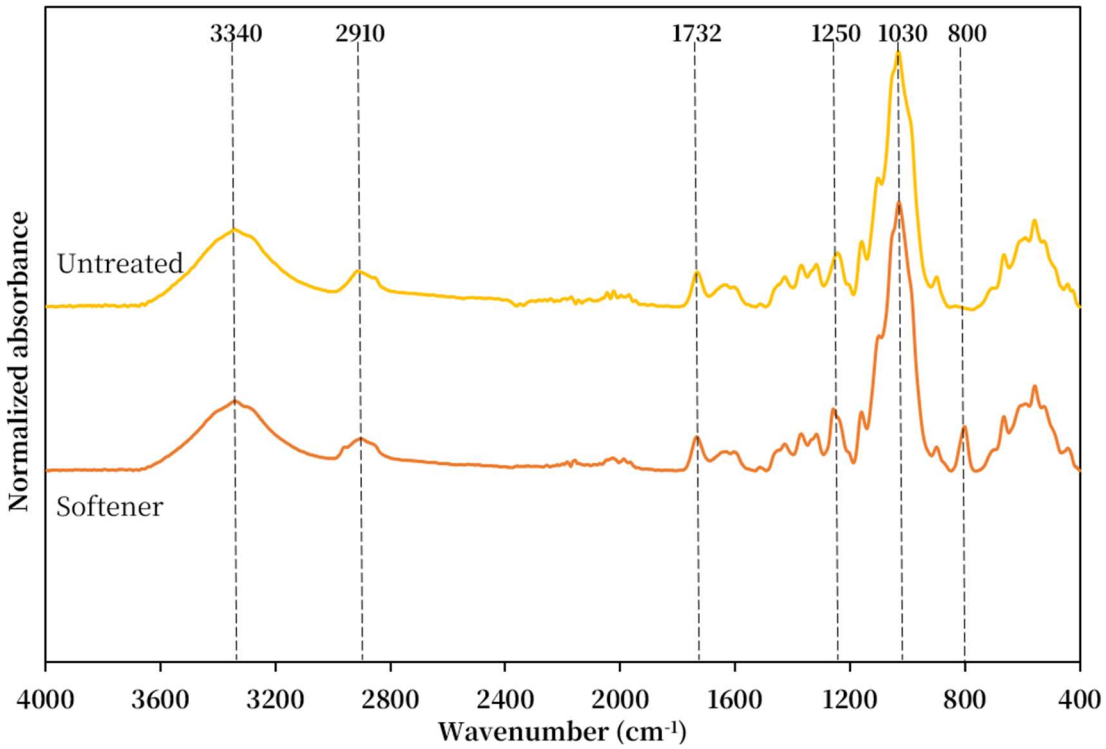

Figure 4. FTIR spectrum of untreated and softener-treated PALF.

The presence of silicone-related extractives on the fiber surface influenced surface smoothness, flexibility, and inter-fiber friction reduction, leading to reduced fiber stiffness and improved fiber dispersion in the polymer or textile blends, and enhancing processability and handling performance. These findings concurred with previous studies reporting that silicone-based finishes improved the tactile and mechanical

behavior of natural fibers without altering their intrinsic chemical composition [39]. The presence of surface coatings altered the light-absorption properties of dyed fibers, affecting color uniformity and depth. Improved dye absorption in PALF-S enhanced the visual integration with cotton fibers, an important aspect for textile aesthetic and functional properties. The cocoa leaf dye adhered more effectively to the softened PALF, due to increased fiber porosity or changes in surface energy caused by the softener coating. These findings concurred with studies on natural fiber dyeing enhancements achieved through pretreatment modifications [34,35], emphasizing the importance of fiber surface engineering in achieving consistent and vibrant coloration in blended textiles.

The fiber fineness and mechanical properties of PALF-U and PALF-S are summarized in Table 1. The increase in fiber thickness after softener treatment suggested that the treatment coated the fiber surface, thereby influencing its mechanical behavior, while the increase in toughness in PALF-S, as noted by Ismoilov et al. (2019) [13], indicated that the softener application enhanced fiber flexibility, reducing brittleness and improving fiber spinning processability for textile applications. This lubricating effect prevented breakage during high-stress processes like spinning by allowing the fibers to slide over each other more easily [40]. This effect is particularly relevant for coarse and stiff fibers like PALF, which typically exhibit high tenacity (23 cN/Tex in PALF-U) but lower flexibility. The improvement in fiber toughness without a significant loss in strength made the softener-treated PALF more adaptable for use in blended yarns and composite textiles.

Table 2 shows the color strength (K/S) and CIE L*a*b* values of cotton and pineapple fibers before and after cocoa leaf dyeing. The application of a cationic agent prior to dyeing for PALF-S significantly improved dye absorption and fiber charge modification, thereby facilitating improved interaction with natural dyes. Cationic treatments have been widely used to enhance the uptake of anionic dyes by improving fiber polarity, a technique commonly applied to cellulose-based fibers [34]. The observed increase in color strength (K/S values) for PALF-S suggested that the treatment effectively promoted higher dye fixation, as a suitable approach for improving pineapple fiber dyeability. A ferrous sulfate mordant was employed to enhance the color retention in PALF-S. The transition of PALF color toward red (a*) and blue (b*) tones following post-mordanting indicated the development of strong fiber–dye interactions, essential for achieving vibrant and durable coloration in natural fibers [35]. PALF exhibited reduced lightness (L*) and a more pronounced yellow hue (b*) than cotton fibers, with the elevated color strength (K/S) value signifying enhanced dye absorption by the fibers. PALF-S exhibited significant dye absorption at a wavelength of 400 nm. Fiber pretreatment eliminated surface contaminants and increased fiber charge, followed by mordanting with ferrous sulfate.

The ability to quantify color variations between the PALF and cotton fibers enabled a more detailed understanding of fiber positioning and blending efficiency. The higher dye absorption at 400 nm for PALF compared with cotton fibers highlighted the differences in fiber structure and chemical composition, which affected dye penetration and retention. This finding supported the need for fiber-specific dyeing protocols in the development of multi-fiber blended yarns for sustainable textiles.

Table 1. Chemical compositions and fiber characteristics of PALF before (PALF-U) and after softening treatment (PALF-S).

PALF Property	PALF-U	PALF-S
Chemical composition		
Alcohol-benzene solution	4.07	4.27
Alcohol solubility	0.20	0.34
Hot water solubility	0.32	1.31
Total extractives	4.59	5.92
Lignin	3.70	3.68
Holocellulose	88.38	86.94
Alpha-cellulose	67.72	66.30
Hemicellulose	20.66	20.64
Ash content	0.13	0.14
Fiber characteristics		
Diameter (μm)	56.56 ± 9.01	53.07 ± 4.94
Fineness (Tex)	4.01 ± 1.26	3.53 ± 0.68
Tenacity (cN/Tex)	23.33 ± 7.71	27.52 ± 5.92
Elongation (%)	2.36 ± 0.60	2.76 ± 0.57

Table 2. Color strength (K/S) and L* a* b* values of cotton fibers and PALF before and after cocoa leaf dyeing.

Fiber	K/S	L*	a*	b*
Before dyeing				
Cotton fiber	0.22 ± 0.01^{b}	85.09 ± 1.05^{a}	0.19 ± 0.13^{b}	6.33 ± 0.65^{c}
PALF-S	0.76 ± 0.05^{b}	81.20 ± 0.96^{b}	0.30 ± 0.14^{b}	12.49 ± 0.47^{a}
After dyeing				
PALF-S	13.65 ± 1.72^{a}	29.96 ± 1.37^{c}	2.51 ± 0.13^{a}	7.55 ± 0.13^{b}

Different letters (a, b, and c) in the same column indicate that the results are significantly different at $p < 0.05$ by Duncan's Multiple-Range Test. ns: non-significant difference.

Table 3 presents the physical characteristics of PALF and cotton fibers prior to blending. The PALF exhibited a bundled structure, resulting in significantly greater apparent fiber thickness compared with cotton. The diameters of the PALF were two to four times greater than the cotton fibers, consistent with previous findings [13]. Both fibers displayed similar tenacity, consistent with prior studies [4], but the cotton fibers showed superior extensibility, suggesting greater flexibility and elongation potential.

Table 3. Characteristics of PALF and cotton fibers.

Physical property	PALF-S	Cotton fiber
Diameter (microns)	53.07 ± 4.94[a]	22.10 ± 2.69[b]
Length (millimeters)	35.00 ± 5.66[a]	27.00 ± 7.07[b]
Fineness (Tex)	3.53 ± 0.68[a]	0.40 ± 0.40[b]
Tenacity (cN/Tex)	27.52 ± 5.92[ns]	28.95 ± 9.02[ns]
Elongation (%)	2.76 ± 0.57[b]	6.50 ± 3.54[a]

Different letters (a, b, and c) in the same column indicate that the results are significantly different at $p < 0.05$ by Duncan's Multiple-Range Test. ns: non-significant difference.

Fiber diameters are known to influence mechanical properties, particularly strength. Several studies have reported an inverse relationship between fiber diameter and strength, whereby an increase in fiber diameter corresponds to a reduction in strength [6]. This phenomenon was attributed to the stress distribution across the fiber cross-section, with thicker fibers containing a greater number of structural defects or irregularities that adversely affected their load-bearing capacity.

Both PALF and cotton fibers have a cellulose-rich composition, which contributes to their comparable molecular structures [41–43]. The presence of a cellulosic framework in PALF suggested that its properties can be further modified through chemical or mechanical processing to enhance compatibility with cotton fibers in blended yarns. These findings underscore the potential of PALF as a sustainable alternative in textile applications, particularly in eco-friendly fiber blends, with structural and mechanical characteristics optimized for enhanced performance.

The physical and mechanical properties of blended yarns, produced at 5 and 10 Ne yarn counts and incorporating different PALF-to-cotton ratios (0:100, 20:80, 30:70, and 50:50) were assessed to evaluate their performance characteristics, including yarn evenness. As indicated in Figure 5, the 100% cotton yarn exhibited the optimal overall performance in both yarn counts, aligning with previous findings on the superior spinnability and mechanical properties of cotton fibers [14]. Mechanical performance and yarn uniformity decreased with increasing PALF content, suggesting that the intrinsic characteristics of PALF negatively affected fiber cohesion in blended yarns.

PALF are known for their rough, linear morphology and lack of crimp, which significantly affect their behavior in blended yarns. Unlike cotton, which possesses natural crimp that enhances inter-fiber cohesion, PALF exhibit a stiffer, straighter structure, leading to reduced yarn uniformity and mechanical integrity. The 10 Ne blended yarn displayed superior strength and uniformity to the 5 Ne yarn, as shown in Figure 5, with higher tenacity and lower evenness values. This improvement was attributed to the higher fiber contact area in finer yarns, which promoted stronger inter-fiber adhesion, thereby enhancing yarn cohesion and tensile properties.

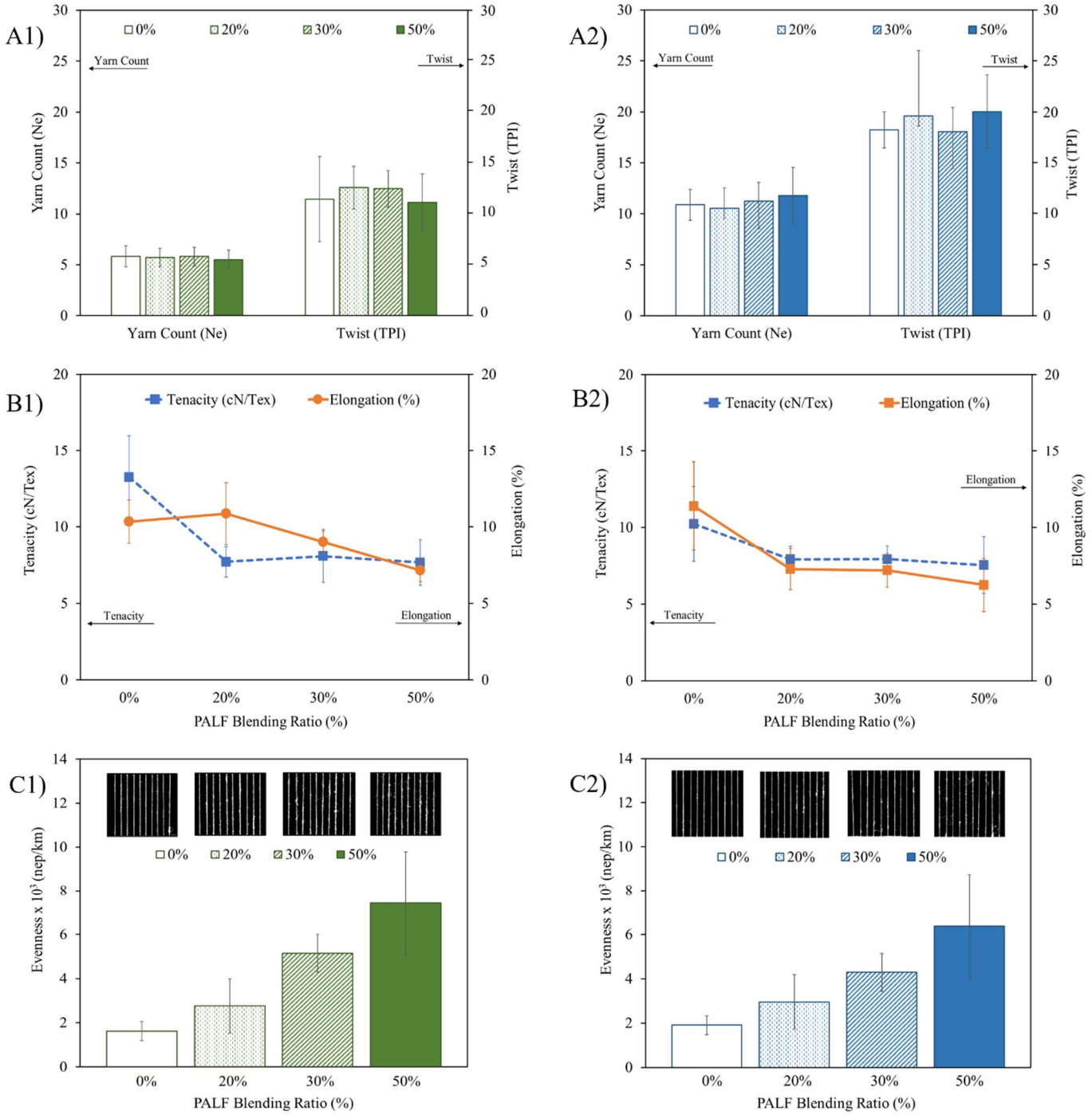

Figure 5. Yarn characteristics of PALF/cotton blends at different PALF blending ratios (0–50%) produced using a ring-spinning machine, showing **(A)** yarn count and twist, **(B)** tenacity and elongation, and **(C)** evenness for **(1)** 5 Ne and **(2)** 10 Ne yarn counts.

The fiber distribution in the yarn cross-section was examined using three morphological characterization methods—optical microscopy, SEM, and SRXTM—with results shown in Figures 6 and 7. Optical microscopy provided the clearest contrast, as the red-colored PALF were easier to distinguish compared with the white cotton fibers. Microscopic analysis of the yarn cross-sections using SEM and SRXTM (Figures 6 and 7) revealed poor bonding between the PALF and cotton fibers, particularly at higher

PALF blend ratios. In the 50% PALF blend, the PALF migrated toward the yarn's outer layer, a phenomenon likely attributable to their coarser diameter and lower inter-fiber compatibility than the cotton fibers. This migration adversely affected the yarn surface quality, leading to increased hairiness, uneven texture, and reduced fabric comfort.

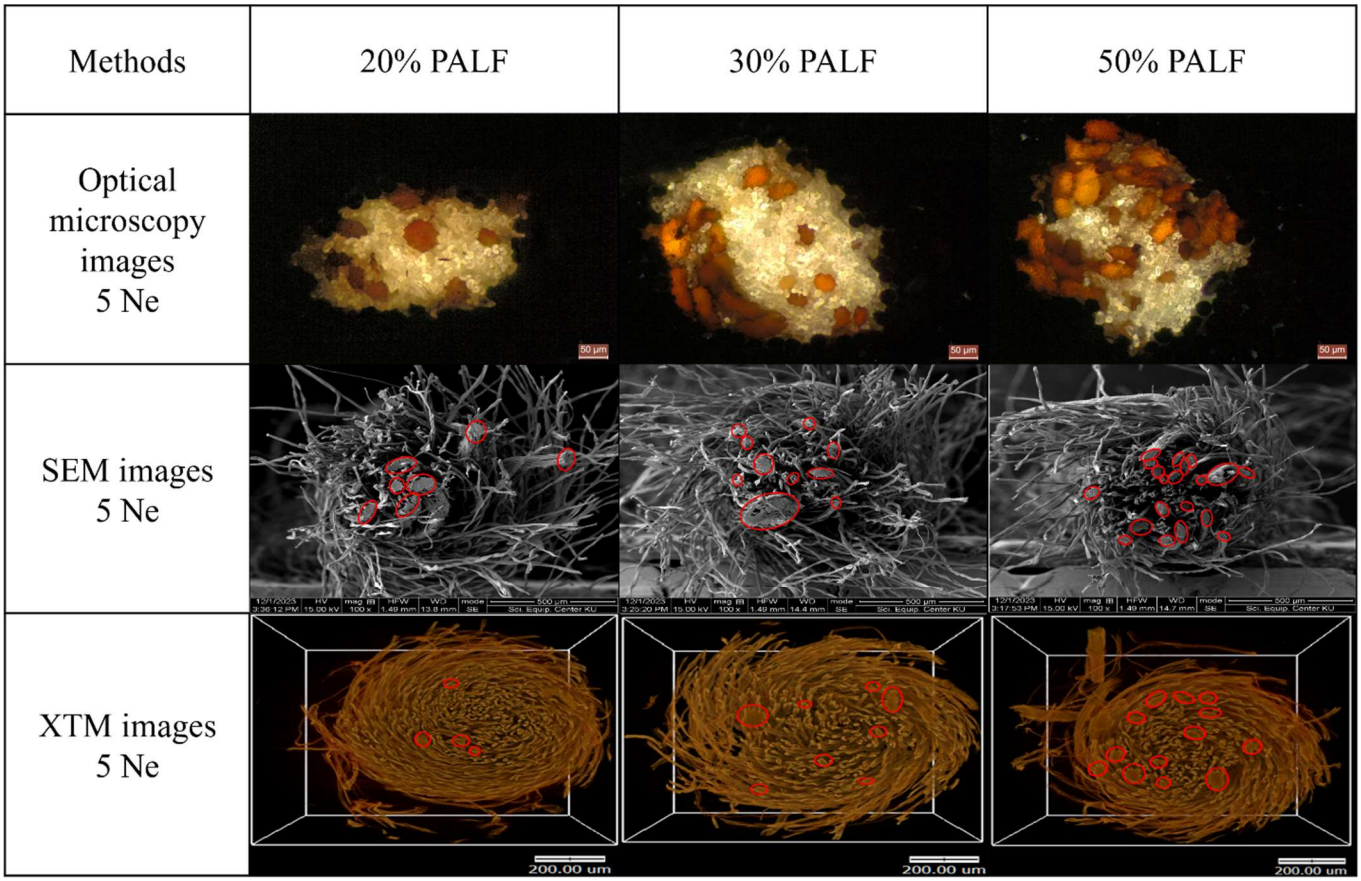

Figure 6. Cross-sectional images of PALF/cotton blended yarns with various PALF contents (20%, 30%, and 50%) at 5 Ne yarn counts obtained by optical microscopy, SEM, and SRXTM. Red markings indicate PALF fiber regions within the yarn structure.

The fiber migration behavior observed in the PALF–cotton yarn blends aligned with theoretical and experimental studies on fiber modulus and yarn structure. Çelik and Gülistan (2023) [44] reported that fibers with a higher Young's modulus (i.e., stiffer fibers) migrated toward the inner regions of the yarn, whereas fibers with a lower Young's modulus (i.e., more flexible fibers) were predominantly concentrated in the yarn's outer regions. This explained why PALF, which exhibited higher stiffness than cotton fibers, migrated within the yarn structure during the spinning process, thereby impacting yarn evenness, strength, and overall performance. These findings highlighted the structural challenges associated with blending PALF with cotton fibers and emphasized the need for fiber modification strategies (e.g., surface treatments or mechanical processing) to enhance compatibility and optimize yarn performance in eco-friendly textile applications.

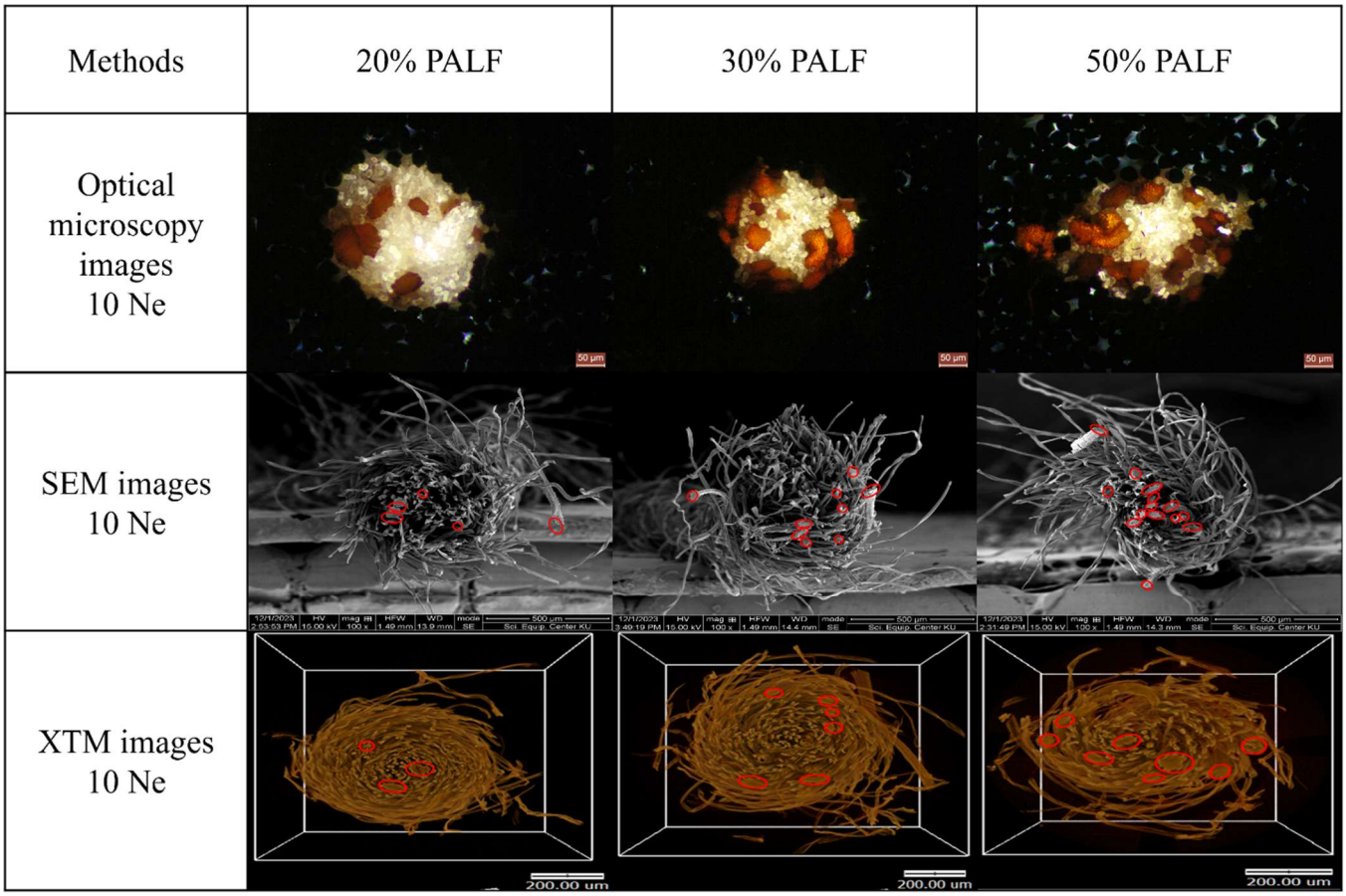

Figure 7. Cross-sectional images of PALF/cotton blended yarns with various PALF contents (20%, 30%, and 50%) at 10 Ne yarn counts obtained by optical microscopy, SEM, and SRXTM. Red markings indicate PALF fiber regions within the yarn structure.

Previous research on silk and cotton fiber blends [8,9] demonstrated that fiber distribution within the yarn cross-section significantly affects fiber migration and mobility within the micro-spinning system [45,46]. These findings suggested that fiber alignment and placement within the yarn structure influenced mechanical behavior and yarn uniformity. In the analysis of yarn counts, the 30:70 PALF–cotton blend exhibited a more uniform distribution of PALF, as revealed by cross-sectional imaging, compared with the other blend ratios. This improved distribution was attributed to a better balance between the cotton matrix and the coarser PALF, allowing for more effective inter-fiber interactions and reducing fiber clumping or migration toward the yarn surface.

The tenacity and elongation of the 20:80 and 30:70 PALF–cotton blends were statistically similar, indicating that increasing the PALF content beyond 20% did not significantly enhance or degrade the tensile performance of the yarn. However, yarn uniformity in the 30:70 blend was superior to the 20:80 blend, due to a higher concentration of PALF on the yarn surface. This surface migration improved fiber cohesion and packing efficiency, thereby reducing the variability in yarn thickness and enhancing yarn evenness during the spinning process.

These findings underscore the importance of fiber distribution in blended yarns, particularly when incorporating stiffer, non-crimped natural fibers such as PALF. A well-balanced blend ratio, such as 30:70, may help mitigate fiber migration issues while maintaining acceptable mechanical properties as a promising composition for eco-friendly textile applications. A detailed examination of the blended spun yarns at varying yarn counts and fiber ratios using optical microscopy, SEM, and SRXTM (Figures 5 and 6) provided critical insights into fiber distribution within the yarn structure. The findings indicated that in coarser 5 Ne yarns, which exhibited a larger diameter, PALF predominantly encircled the yarn's outer regions (Figure 5). By contrast, in the finer 10 Ne yarns (Figure 6), the cotton fibers were more concentrated on the yarn surface, whereas PALF were distributed more toward the yarn core compared with the coarser 5 Ne yarns.

All three imaging techniques—optical microscopy, SEM, and SRXTM—consistently revealed a similar fiber distribution pattern. The PALF migrated toward the yarn core, a phenomenon that became more pronounced with increasing PALF content. This behavior was attributed to the coarser, more rigid nature of PALF compared with cotton fibers, which led to non-uniform dispersion within the yarn structure. Such migration trends aligned with previous studies on fiber positioning in heterogeneous blended yarns, where stiffer, larger-diameter fibers were concentrated in the inner regions due to lower flexibility and reduced twisting conformity [9,45].

SRXTM imaging provided a three-dimensional perspective of the yarn structure, further confirming these findings (Figures 5 and 6). However, material differentiation between PALF and cotton fibers was challenging due to their similar contrast levels in X-ray images. By contrast, SEM images offered a clearer distinction between PALF and cotton fibers; however, the unfixed and loosely packed yarn diameter made it difficult to resolve fiber distribution across individual layers. SRXTM analysis revealed a clockwise Z-twist pattern in the fiber bundles as a critical structural feature influencing yarn strength and cohesion.

These findings highlighted the importance of fiber distribution analysis in predicting yarn quality and mechanical performance, reinforcing the role of advanced imaging techniques in understanding fiber behavior within eco-friendly textile composites. The radial distribution of PALF by weight in blended spun yarns at varying yarn counts and blend ratios was analyzed to assess fiber positioning within the yarn structure. The evaluation considered multiple concentric zones, ranging from the yarn core to the surface, to determine the extent of fiber migration and uniformity. The zoning methodology and sample sectioning employed in this study represent a more precise and less biased approach compared with the fiber migration study conducted by Chollakup et al. (2008) [9]. They estimated fiber positioning by dividing the yarn perimeter into zones and reducing the area by 20% per zone, possibly leading to inconsistent

fiber count distributions across zones. By contrast, the refined zoning technique used in this study ensured a more uniform assessment of PALF and cotton fiber distribution, particularly in blends containing fibers with significantly different diameters.

Figure 8 presents the radial distribution of PALF in cotton blends, analyzed using the IBI across various yarn counts and blend ratios for all cross-sectional determination methods. An IBI value approaching 1 indicates an ideal and uniform fiber distribution, whereas values below 1 suggest cotton-dominated regions and values above 1 imply a higher concentration of PALF in the respective zone. For the coarser 5 Ne yarns (Figure 8A1–C1), the IBI values obtained using all three methods were lower at the yarn core, indicating a higher concentration of cotton fibers in the central region. Moving outward toward zones 21–44, the IBI values increased, particularly in yarns containing 20% and 30% PALF. This phenomenon was attributed to the significant size difference between PALF and cotton fibers, whereby the larger PALF migrated outward, leading to uneven fiber distribution and IBI values exceeding unity. At the outermost yarn surface, elevated IBI values persisted at 20% and 30% PALF contents, indicating fiber accumulation at the periphery. However, at a 50% PALF concentration, the fibers were more evenly distributed throughout the cross-section, as reflected by an IBI value below 1.5. This uniformity was further corroborated by microscopic cross-sectional images (Figure 6), which visually demonstrated a more homogeneous fiber distribution at higher PALF contents.

For the finer 10 Ne yarns (Figure 8A2–C2), results obtained using all three methods showed that the yarn core remained predominantly composed of cotton fibers, facilitating more uniform dispersion up to zone 40. Toward the outer regions, the IBI values exceeded 1, mirroring the trends observed in the 5 Ne yarns. This outward migration of PALF suggested that larger and stiffer fibers accumulated at the yarn surface, a common trend in blended yarns with heterogeneous fiber compositions [9].

With increasing PALF content, yarn uniformity diminished, particularly in coarser yarns due to enhanced fiber migration. However, the tensile strength remained unaffected, indicating that fiber migration did not significantly compromise the overall mechanical integrity of the yarns. The total IBI value for the 10 Ne yarn was lower than the 5 Ne yarn, with values closer to 1, suggesting a more random and uniform fiber distribution throughout the yarn structure. The analysis further confirmed that PALF dispersion was more pronounced at the yarn surface than at the core, reinforcing the importance of fiber size and morphology in governing blended yarn behavior.

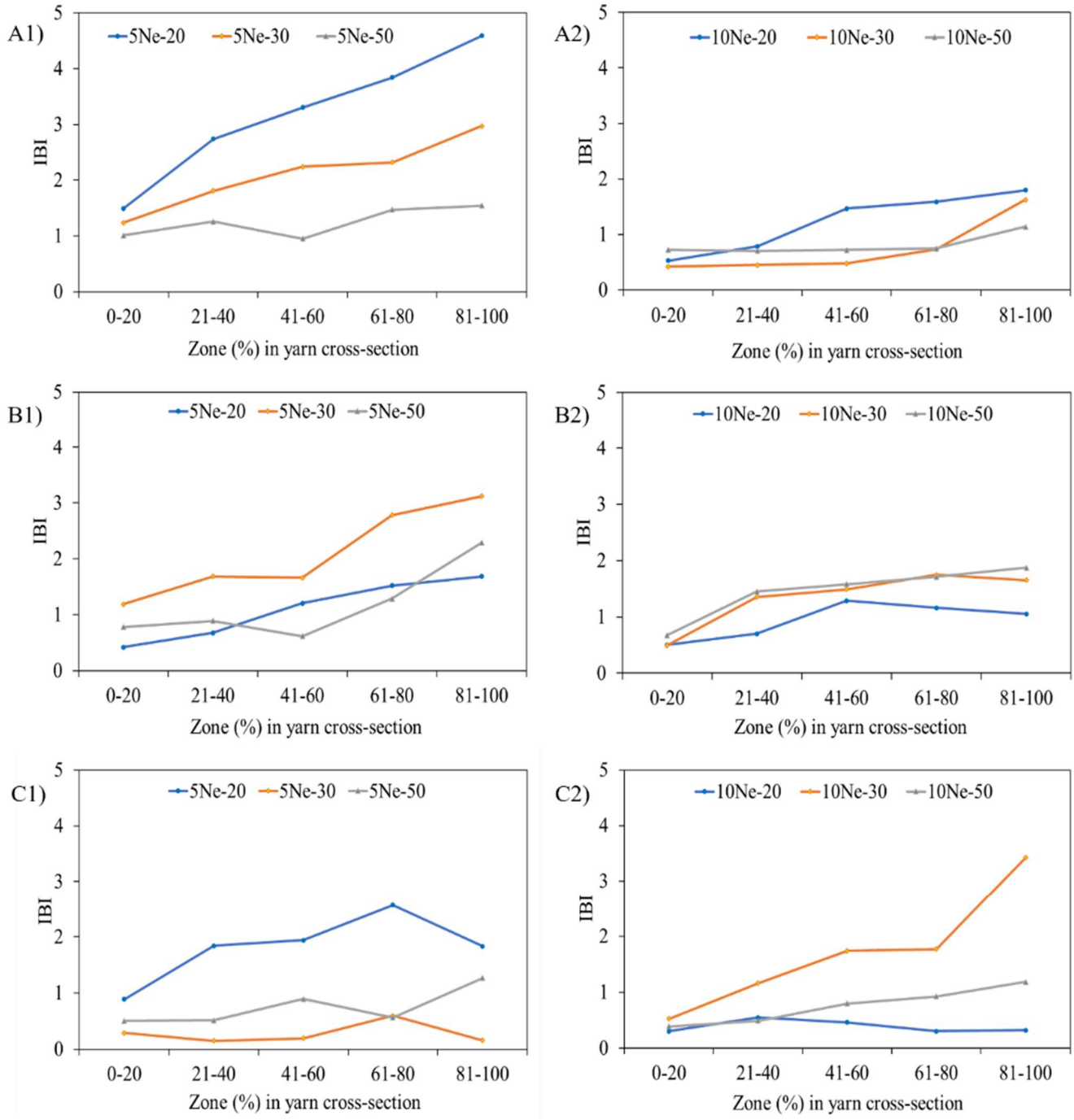

Figure 8. IBI values across different zones in yarn cross-sections, determined using three methods: **(A)** optical microscopy, **(B)** SEM, and **(C)** SR-XTM for two yarn counts: **(1)** 5 Ne and **(2)** 10 Ne.

The blending irregularity model proposed in this study offered a predictive framework for optimizing fiber blending parameters, particularly in PALF–cotton yarns [20,47]. As the yarn count increased from 5 to 10 Ne, the yarn became finer, leading to a reduction in packing density. By contrast, coarser yarns contained a greater number of fibers per cross-section, subjecting them to higher compressive forces and resulting in increased packing density [44]. These findings highlighted the structural variations in blended yarns and emphasized the critical role of

fiber morphology and yarn count in determining yarn properties for eco-friendly textile applications.

At the same PALF–cotton fiber ratio of 50:50, cross-sectional analyses of 5 Ne blended yarns using optical microscopy, SEM, and SRXTM demonstrated similar uniform fiber distributions, resulting in IBI values below 1 within the 60% zone (Figure 9A). However, for the finer 10 Ne blended yarns, only the IBI values derived from optical microscopy and SRXTM images indicated similar uniform fiber distributions (IBI < 1) across all yarn cross-sectional zones, whereas the SEM images indicated lower uniformity (Figure 9B). This suggested that SRXTM imaging was more suitable for precise and rapid yarn cross-sectional analysis compared to optical microscopy. Nevertheless, the SRXTM technique, which incorporates synchrotron radiation, may serve as a more advanced approach in future studies, particularly for applications involving color or surface characterization.

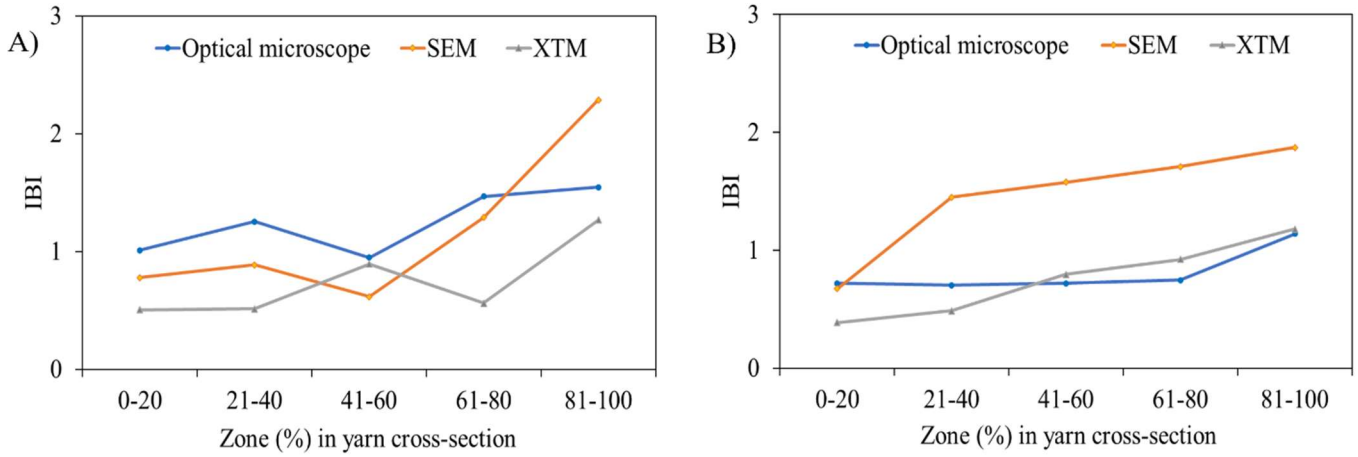

Figure 9. Comparison of IBI values across different zones in the yarn cross-section determined using three methods for two yarn counts: (**A**) 5 Ne and (**B**) 10 Ne at 50% PALF content.

In terms of spinning performance, the PALF exhibited lower flexibility and cohesion than conventional cotton fibers, which limited yarn strength and increased end breakage during spinning. From an industrial perspective, additional upstream controls will be required to ensure stable processing of PALF-containing blends. Consistent PALF cleaning (e.g., removal of residual pith, waxy/extractive impurities, and decortication residues) is critical because contaminants increase nep formation, impair carding efficiency, and exacerbate yarn irregularity. Tighter control of PALF fiber-length distribution (via standardized cutting, opening, and removal of excessive short fibers) will be necessary to reduce preferential loss during carding/drafting and improve interfiber cohesion during high-speed ring-spinning. Implementing such preprocessing steps, together with optimized drafting and twist insertion, would improve the industrial compatibility of PALF–cotton blends and enhance reproducibility under higher spindle speeds and stricter quality tolerances. Surface treatments, such as silicone softening, and optimization of twist levels can partially

mitigate these issues; however, further process optimization is required to achieve stable, high-speed operation. The compatibility of PALF blends with high-speed ring-spinning systems remains a key consideration. Laboratory-scale spinning demonstrated feasibility, but industrial ring-spinning operates at significantly higher spindle speeds with stricter quality tolerances. The adaptation of process parameters, including draft ratios, twist insertion, and traveler selection is essential to accommodate PALF-containing blends without compromising productivity or yarn quality. These challenges must be addressed before upgrading PALF-based yarns from laboratory-scale feasibility to sustainable industrial-scale production.

CONCLUSIONS

This study demonstrated the valorization of pineapple leaf agro-residues into bio-based PALF–cotton ring-spun yarns and clarified the microstructure–property relationships governing their performance. PALF were mechanically extracted, softened, and naturally dyed with cocoa leaves to enhance processing and enable visual discrimination within blended yarn cross-sections. The PALF were then blended with cotton fibers at ratios of 0:100, 20:80, 30:70, and 50:50 and spun into 5 and 10 Ne yarns using a conventional laboratory-scale ring-spinning system. The results revealed that the mechanical properties, including tensile strength and elongation, exhibited minimal variation among the 20%, 30%, and 50% PALF blends, with the exception of yarn evenness. Increasing PALF content led to reduced yarn uniformity, which was attributed to the coarser and more rigid morphology of PALF. The limited crimp and higher stiffness of PALF promoted migration toward the yarn periphery. Cross-sectional fiber analysis conducted using three independent methods confirmed this trend, with IBI values exceeding 1, indicating heterogeneous fiber dispersion. By contrast, cotton fibers were predominantly located within the yarn core, producing IBI values below 1. The findings were corroborated using SEM and SRXTM and further validated through optical microscopy observations of fiber distribution. Based on the SRXTM results, yarn cross-sectional analysis was faster than optical microscopy and provided greater precision, with further image analysis incorporating color and cross-sectional features.

In summary, increasing PALF content adversely influenced yarn uniformity and mechanical integrity, underscoring the necessity of optimizing blend ratios for enhanced yarn performance. Our study provides valuable insights into the structural behavior and fiber distribution mechanisms of natural fiber blends, and contributes to the advancement of sustainable yarn manufacturing within the framework of environmentally responsible textile production.

DATA AVAILABILITY

All the generated and analyzed datasets presented in this study are available from the corresponding author upon reasonable request.

AUTHOR CONTRIBUTIONS

Conceptualization, NR and RC; methodology, RC and RM; formal analysis, TA and WS; investigation, TA and RC; resources, RR; data curation, TA, PP and PO; writing—original draft preparation, TA, RC and NR; writing—review and editing, NC and NR; supervision, RC; project administration, PO and JB; All the authors have read and agreed to the published version of the manuscript.

CONFLICTS OF INTEREST

The authors declare that they have no conflicts of interest.

FUNDING

This research was funded by Kasetsart University Research and Development Institute (KURDI), Project FF(KU)20.66.

ACKNOWLEDGMENTS

This research is a subproject under the program “Innovative of Pineapple Leaf Utilization for Developing Sustainable Green Agricultural Community Enterprise” led by Pawarin Tuntariyanond, Faculty of Agro-industry, Kasetsart University. The authors would like to express their sincere appreciation to the program for its support and coordination, which enabled the successful implementation of this research.

REFERENCES

1. Phuangsubsin C, Jantakard H, Vinitpittayakul K. Risk assessment of sustainable pineapple supply chain management. Thai Environ Eng J. 2024;38(1):1-11.
2. Apipatpapha T, Ongkunaruk P, Chollakup R. Pineapple leaf fiber supply chain analysis for the sustainability of community enterprise: a case study in Thailand. IOP Conf Ser Earth Environ Sci. 2022;1074:012032. doi: 10.1088/1755-1315/1074/1/012032
3. Suphamitmongkol W, Khanoonkon N, Rungruangkitkrai N, Boonyarit J, Changniam C, Sampoompuang C, et al. Potential of pineapple leaf fibers as sound and thermal insulation materials in Thailand. Prog Appl Sci Tech. 2023;13(1):26-32. doi: 10.14456/past.2023.5
4. Hazarika P, Hazarika D, Kalita B, Gogoi N, Jose S, Basu G. Development of apparels from silk waste and pineapple leaf fiber. J Nat Fibers. 2018;15(3):416-24. doi: 10.1080/15440478.2017.1333071

5. Jalil MA, Moniruzzaman M, Parvez MS, Siddika A, Gafur MA, Repon MR, et al. A novel approach for pineapple leaf fiber processing as an ultimate fiber using existing machines. Heliyon. 2021;7:e07861. doi: 10.1016/j.heliyon.2021.e07861
6. Jose S, Salim R, Ammayappan L. An overview on production, properties, and value addition of pineapple leaf fibers (PALF). J Nat Fibers. 2016;13:362-73. doi: 10.1080/15440478.2015.1029194
7. Jalil MA, Sinha RC, Mahabubuzzaman A, Milon Hossain M, Idris MA. Study on physical and structural properties of jute-palf blended yarn spun by apron draft spinning. Res J Text Appar. 2015;19:9–15. doi: 10.1108/RJTA-19-03-2015-B002
8. Chollakup R, Sinoimeri A, Osselin JF, Frydrych R, Drean JY. Silk waste/cotton blended yarns in cotton microspinning: physical properties and fiber arrangement of blended yarn. Res J Text Appar. 2005;9:57-69. doi: 10.1108/RJTA-09-04-2005-B006
9. Chollakup R, Osselin JF, Sinoimeri A, Drean JY. Effects of blending parameters on the cross-section fiber migration of silk/cotton blends. Text Res J. 2008;78:361-9. doi: 10.1177/0040517508089758
10. Mahmud H, Akter S, Islam S. Surface modification and characterization of raw pineapple leaf fibers (PLF) using sodium hydroxide (NaOH) and graphene oxide (GO). Fibers Polym. 2025;26:337-51. doi: 10.1007/s12221-024-00794-z
11. Vaithanomsat P, Trakunjae C, Meelaksana J, Boondaeng A, Apiwatanapiwat W, Janchai P, et al. Improvement of pineapple leaf fiber quality by pectinase produced from newly isolated *Bacillus subtilis* subsp. *inaquosorum* P4-1. Fibers Polym. 2022;23:576-88. doi: 10.1007/s12221-021-0120-0
12. Chollakup R, Sinoimeri A, Philippe F, Schacher L, Adolphe D. Tactile sensory analysis applied to silk/cotton knitted fabrics. Int J Cloth Sci. Technol. 2004;16(1-2):132-40. doi: 10.1108/09556220410520423
13. Ismoilov K, Chauhan S, Yang M, Heng Q. Spinning system for pineapple leaf fiber via cotton spinning system by solo and binary blending and identifying yarn properties. J Text Sci Technol. 2019;5:86-91. doi: 10.4236/jtst.2019.54008
14. Azihar AA, Roslan MN. Yarn properties of blended fiber pineapple leaf fiber/cotton. Prog Eng Appl Technol. 2023;4(2):491-8.
15. Sethupathi M, Khumalo MV, Skosana SJ, Muniyasamy S. Recent developments of pineapple leaf fiber (PALF) utilization in polymer composites: a review. Separations. 2024;11(8):245. doi: 10.3390/separations11080245
16. Duangsuwan S, Amornsakchai T, Phinyocheep P, Thanawan S. Achieving high-performance green composites from pineapple leaf fiber–poly(butylene succinate) through both fiber alignment and matrix orientation across the thickness. ACS Omega. 2023;8:35693-705. doi: 10.1021/acsomega.3c02690
17. Abdelkader M, Mazari A, Zafar S. Experimental techniques to obtain the cross-sectional images of textile yarns. Materials. 2022;15(14):4726. doi: 10.3390/ma15144726

18. Grishanov SA, Lomov SV, Cassidy T, Harwood RJ. The simulation of the geometry of a two-component yarn. Part II: fiber distribution in the yarn cross-section. J Text Inst. 1997;88:352-72. doi: 10.1080/00405000.1997.11090889
19. Cao Q, Zhou Y, Yu C. Application of image processing technology on testing blending ratio and blending irregularity of blended yarns. Text Res J. 2023;93:3945-55. doi: 10.1177/00405175231168420
20. Zeidman M, Sawhney PS. Influence of fiber length distribution on strength efficiency of fibers in yarn. Text Res J. 2002;72:216-20. doi: 10.1177/004051750207200306
21. Gharehaghaji AA, Moghassem A. Redistribution of fibers in the structure of hollow ring spun yarn. Int J Eng. 2009;22:197-204.
22. Atalie D, Ferede A, Rotich GK. Effect of weft yarn twist level on mechanical and sensorial comfort of 100% woven cotton fabrics. Fashion Text. 2019;6:3. doi: 10.1186/s40691-018-0169-6
23. Yu XW, Wang H, Wang ZW. Analysis of yarn fiber volume fraction in textile composites using scanning electron microscopy and X-ray micro-computed tomography. J Reinf Plast Compos. 2019;38:199-210. doi: 10.1177/0731684418811943
24. El-Din Al-Mofty S, Elghazawy NH, Azzazy HME. A one-step facile process for extraction of cellulose from rice husk and its use for mechanical reinforcement of dental glass ionomer cement. RSC Sustain. 2023;1:1743-50. doi: 10.1039/D3SU00230F
25. Brunsek R, Jugov N, Marasovic P, Mioč A. Biodegradation properties of natural fibers for agro textile nonwovens production. IOP Conf Ser Mater Sci Eng. 2023;1266:012017. doi: 10.1088/1757-899X/1266/1/012017
26. Khantayanuwong S, Yimlamai P, Chitbanyong K, Wanitpinyo K, Pisutpiched S, Sungkaew S, et al. Fiber morphology, chemical composition, and properties of kraft pulping handsheet made from four Thailand bamboo species. J Nat Fibers. 2023;20:2150924. doi: 10.1080/15440478.2022.2150924
27. Serra-Parareda F, Tarrés Q, Espinach FX, Vilaseca F, Mutjé P, Delgado-Aguilar M. Influence of lignin content on the intrinsic modulus of natural fibers and on the stiffness of composite materials. Int J Biol Macromol. 2020;155:81-90. doi: 10.1016/j.ijbiomac.2020.03.160
28. Harwood R, Smith E. Testing of natural textile fibers. In: Handbook of Natural Fibers. Amsterdam (the Netherlands): Elsevier; 2020. p. 535-576. doi: 10.1016/B978-0-12-818398-4.00017-7
29. Rungruangkitkrai N, Mongkholrattanasit R, Ounu P, Chartvivatpornchaia N, Boonyarit J, Laohaphatanaleart K, et al. Enhancing sustainable silk textiles: optimization of teak leaf extract dyeing and antibacterial efficacy. Curr Res Green Sustain Chem. 2025;10:100457. doi: 10.1016/j.crgsc.2025.100457
30. Atav R, Dilden DB, Keskin S, Ergünay U. Investigation of the dyeability and various performance properties of fabrics produced from flax and hemp fibers and their blends with cotton in comparison with cotton. Color Technol. 2024;140:440-450. doi: 10.1111/cote.12720

31. Coplan MJ, Bloch MG. A study of blended woolen structures: Part II: Blend Distribution in Some Wool-Nylon and Wool-Viscose Yarns. Text Res J. 1955;25:902-22. doi: 10.1177/004051755502501102
32. Krucińska I. Fiber blending irregularities in cross sections and on yarn surfaces in relation to yarn properties. Text Res J. 1988;58:291-8. doi: 10.1177/004051758805800508
33. Li C, Shao R, Wang C, Fu G, Yang B. Influence of hemp fiber softening treatment and blend ratio on quality characteristics of hemp-based ternary blended yarn. Fibers Polym. 2023;24:3481-8. doi: 10.1007/s12221-023-00327-0
34. Corrente GA, Scarpelli F, Caputo P, Rossi CO, Crispini A, Chidichimo G, et al. Chemical–physical and dynamical–mechanical characterization of *Spartium junceum* L. cellulosic fiber treated with softener agents. Sci Rep. 2021;11:35. doi: 10.1038/s41598-020-79568-5
35. Jalalah M, Khaliq Z, Ali Z, Ahmad A, Qadir MB, Afzal A, et al. Preliminary studies on conversion of sugarcane bagasse into sustainable fibers for apparel textiles. Sustainability. 2022;14:16450. doi: 10.3390/su142416450
36. Chruściel JJ. Modifications of textile materials with functional silanes, liquid silicone softeners, and silicone rubbers—A Review. Polymers. 2022;14(20):4382. doi: 10.3390/polym14204382
37. Smith AL. The analytical chemistry of silicones. New York (NY, US): Wiley-Interscience; 1991.
38. Fengel D, Wegener G. Wood: chemistry, ultrastructure, reactions. Berlin (Germany): Walter de Gruyter; 1984.
39. Xu Y, Yin H, Yuan S, Chen Z. Film morphology and orientation of amino silicone adsorbed onto cellulose substrate. Appl Surf Sci. 2009;255:8435-42. doi: 10.1016/j.apsusc.2009.05.149
40. Gong RH, Bhatia A. Effects of softeners on mechanical properties of cotton fabric. Res J Text Appar. 2009;13:45-50. doi: 10.1108/RJTA-13-04-2009-B006
41. Asim M, Abdan K, Jawaid M, Nasir M, Dashtizadeh Z, Ishak MR, et al. A review on pineapple leaves fiber and its composites. Int J Polym Sci. 2015;2015:950567.
42. Mishra S, Mohanty AK, Drzal LT, Misra M, Hinrichsen G. A review on pineapple leaf fibers, sisal fibers and their biocomposites. Macromol Mater Eng. 2004;289:955-74. doi: 10.1002/mame.200400132
43. Omojasola PF, Jilani OP, Ibiyemi SA. Cellulase production by some fungi cultured on pineapple waste. Nat Sci. 2008;6:64-79.
44. Çelik Hİ, Gülistan C. Effect of yarn physical properties on fiber migration and packing density of cotton/acrylic blended yarns. Tekstil ve Konfeksiyon. 2023;33:15-26. doi: 10.32710/tekstilvekonfeksiyon.928965
45. Soltani P, Johari MS. A study on siro-, solo-, compact-, and conventional ring-spun yarns. Part I: structural and migratory properties of the yarns. J Text Inst. 2012;103:622-8. doi: 10.1080/00405000.2011.595567
46. Zheng S, Zou Z, Shen W, Cheng L. A study of the fiber distribution in yarn cross section for vortex-spun yarn. Text Res J. 2012;82:1579-86. doi: 10.1177/0040517511431315

47. Cao Q, Qian L, Li H, Yu C. Simulation of sliver blending and evaluation of blending irregularity. Text Res J. 2022;92:2895-908. doi: 10.1177/00405175211028803

How to cite this article:
Rungruangkitkrai N, Apipatpapha T, Chartvivatpornchai N, Boonyarit J, Suphamitmongkol W, Ounu P, et al. Valorization of Pineapple Leaf Agro-Residues into Bio-Based Ring-Spun Yarns: Microstructural Mapping and Mechanical Behavior of PALF–Cotton Blends. J Sustain Res. 2026;8(2):e260046. https://doi.org/10.20900/jsr20260046.